

Early Tests of Scale Invariance in High-Energy Muon Scattering*

D. J. Fox,† C. Chang, K. W. Chen, A. Kotlewski, and P. F. Kunz‡
Physics Department, Michigan State University, East Lansing, Michigan 48824

and

L. N. Hand, S. Herb, S. C. Loken, A. Russell,§ and Y. Watanabe
Laboratory of Nuclear Studies, Cornell University, Ithaca, New York 14850

and

W. Vernon
Physics Department, University of California, San Diego, La Jolla, California 92037

and

M. Strovink||
Joseph Henry Laboratories, Princeton University, Princeton, New Jersey 08540
 (Received 1 August 1974)

Data are presented on deep inelastic scattering of 56.3- and 150-GeV μ^+ from an iron target at the Fermi National Acceleratory Laboratory. Observed event rates, averaged over a wide range in ω , are compared to scale-invariance predictions for q^2 up to 44 (GeV/c)². The ratio of the 150-GeV data to the scale-invariance prediction versus q^2 is not constant for all accepted ω values. A fit of the form $(1 + g^2/\Lambda^2)^{-2}$ yields a lower limit of $\Lambda > 10$ GeV with 90% confidence, averaged over a restricted ω range.

Some years ago, Bjorken predicted¹ that the structure functions in the deep inelastic scattering of leptons from nucleons, although nominally functions of two variables, q^2 and ω ,² would actually, in the limit $q^2/\nu^2 \rightarrow 0$, be functions of ω only. This prediction and the subsequent experimental evidence for its validity discovered at Stanford Linear Accelerator Laboratory (SLAC)³ led to many predictions based on a hypothetical pointlike character of the constituents of the proton and neutron, usually called the parton model.⁴ The experiment reported here extends the scaling test in q^2 and ω using high-energy muons scattered from an iron target at the Fermi National Accelerator Laboratory.

The test of scaling is made by comparing distributions of kinematic quantities at two incident muon energies, 56.3 and 150 GeV, using a large-aperture spectrometer which changes with energy so as to keep ω acceptance and resolution constant. The realization of the scaling geometries is shown in Fig. 1. Longitudinal distances scale as $\sqrt{E_0}$; q^2 and E' scale as E_0 . The counting rate scales as E_0^{-1} and is compensated by scaling the target material (233 g/cm² at 56.3 to 622 g/cm² at 150 GeV). Relative momentum resolution of 14% is held constant by using three degaussed magnets as extra scattering material in the 150-GeV configuration. The total magnetic field inte-

gral scales as $\sqrt{E_0}$ ($\langle P_{\perp} \rangle = 1.3$ or 2.2 GeV/c) and is known to 1% with an uncertainty of 0.5% in its variation over the radius. A scattered-muon trigger is defined by three scintillation counter banks, SA, SB, and SC in Fig. 1, having a hole in the center to prevent beam triggers. A fourth bank of counters, HV₂, is placed upstream of the target to veto accidental beam-halo coincidences. The beam size at the target is sharply defined by another veto, HV₁. Beam muons or muons scattered through very small angles are vetoed by a coincidence of two veto counters labeled BV and BV'. Only information in SC₁₁₋₁₅ has been used in event reconstruction to avoid bias due to showers. The data are presented in several ways in order to investigate stability with respect to differing assumptions as shown in Fig. 2. Scaling the apparatus at each energy is designed to cause the ratio of yields at 150 and 56.3 GeV to be unity if scale invariance holds. The chief scale-noninvariant change in running conditions was the 20% larger diameter of the 56.3-GeV beam. To compensate approximately, the accepted region of the beam was reduced in size by a 4.5-cm radius and 1-mrad angle cut at each energy. Muon flux changes caused by beam cuts were computed using a sample of random beam tracks collected as an auxiliary trigger during running. The resulting "small-beam" scattering yields are shown in

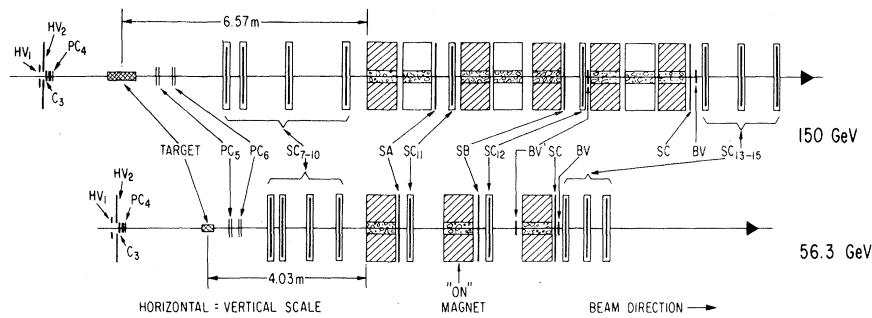


FIG. 1. Apparatus for the scaling test. Shaded magnets are on, others are degaussed. The spark-chamber modules have four planes each and are labeled SC_i . Multiwire proportional chambers of two planes each are shown as PC ; upstream PC and scintillation counters are not shown.

Fig. 2(a) [2(b)] for $E_0 = 150$ (56.3) GeV, plotted in q^2 bins of 4 (1.5) $(\text{GeV}/c)^2$. The 150/56.3 ratio appears in Fig. 2(f). The mean ω varies from 20 in the lowest q^2 bin to 2.5 in the highest bin. This test of scaling is independent of assumptions on the form of $\nu W_2(\omega)$ and can be biased only by certain small residual scale-noninvariant effects in the apparatus or analysis.⁵

Data are also compared to a Monte Carlo calculation based on SLAC-Massachusetts Institute of Technology (MIT) fits⁶ to νW_2^p and νW_2^d with $R = 0.18$.⁷ Known physical effects of any consequence are incorporated into the Monte Carlo calculation, including Fermi motion⁸ in the iron nucleus, muon energy loss, Coulomb scattering in material, radiative corrections, and measuring errors. The 150-GeV data and Monte Carlo yields are shown in Figs. 2(c) and 2(d), and their ratio in Fig. 2(g).⁹ The enhancement at low q^2 is attributed to large- ω events [$\langle \omega \rangle \sim 20$] outside the SLAC q^2 range. The result of removing events having $\omega > 9$ is shown in Fig. 2(h). Since high- q^2 events come from a lower ω region, they are not affected by this cut. Direct comparison with SLAC-MIT results⁶ in their kinematic region yields agreement within 10%.¹⁰ This result supports further μ - e universality.¹¹ The ratio of 56.3-GeV data to SLAC with no constraint is plotted in Fig. 2(i).

To parametrize the sensitivity of the data to possible violations of scale invariance, the ratios in Figs. 2(f)–2(i) are fitted by a “propagator” term in the cross section of the form $N/(1+q^2/\Lambda^2)^2$ (Table I) in three ways: (a) $\Lambda^{-2} = 0$ and N is allowed to vary. (b) Both Λ^{-2} and N are allowed to vary. This procedure allows Λ^{-2} to parametrize a q^2 dependence of the ratio, corresponding to a deviation from unity at high q^2 or at low q^2 or

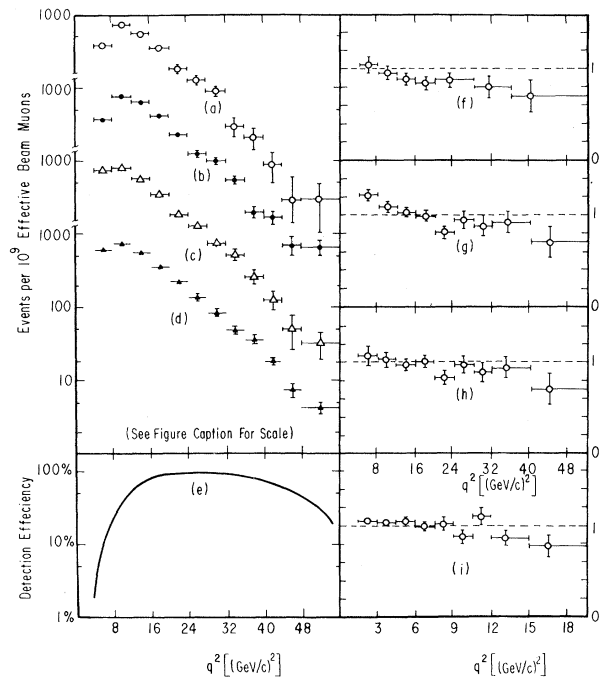


FIG. 2. Data for the scaling test. Muon scattering yields per 10^9 beam muons are plotted for (a) 150-GeV small beam, (b) 56-GeV small beam, (c) 150-GeV full beam, and (d) Monte Carlo (MC) calculation for 150-GeV full beam. Bins in q^2 are 4 (1.5) $(\text{GeV}/c)^2$ for 150- (56-) GeV data; the highest bin contains all data above 48 (18) $(\text{GeV}/c)^2$. The absolute acceptance versus q^2 is shown in (e) (Ref. 13). Yield ratios are plotted for (f) (150-GeV data)/(56.3-GeV data) (a/b); (g) (150-GeV data)/(MC calculation) (c/d); (h) same as (g) with $\omega > 9$; and (i) (56.3-GeV data)/(MC calculation). For ratios of 150- to 56.3-GeV data, the range of q^2 is indicated for the 150-GeV data; the 56.3-GeV q^2 are smaller by a factor of 3/8. Indicated errors are statistical only. The mean ω varies from 20 in the lowest q^2 bin to 2.5 in the highest bin. Ratio of yields is unity if scale invariance holds.

TABLE I. Fits to the ratio of rates as a function of q^2 .

	Constant		$N(1+q^2/\Lambda^2)^{-2}$			$N(1+q^2/\Lambda^2)^{-2}$ ^a			Ref. Fig. 2
	N	Confidence level (%)	N	$\Lambda^{-2} \times 10^4$ (GeV ⁻²)	Confidence level (%)	N	$\Lambda^{-2} \times 10^4$ (GeV ⁻²)	Confidence level (%)	
150 (All ω)	1.02 ± 0.02	0.03	$1.30^{+0.08}_{-0.07}$	83^{+22}_{-20}	59	0.008	(g)
<u>Data</u> 150 MC ($\omega < 9$)	0.95 ± 0.03	40	$1.11^{+0.09}_{-0.08}$	44^{+24}_{-21}	83	$0.96^{+0.027}_{-0.027}$	6^{+10}_{-10}	40	(h)
56.3 (All ω)	1.02 ± 0.02	3	$1.11^{+0.03}_{-0.03}$	74^{+26}_{-24}	48	0.34	(i)
			$N \left(\frac{1+\lambda q^2/\Lambda^2}{1+q^2/\Lambda^2} \right)^{2b}$			$N \left(\frac{1+\lambda q^2/\Lambda^2}{1+q^2/\Lambda^2} \right)^{2a,b}$			
<u>Data</u> 150/56.3 Data (All ω)	0.90 ± 0.03	43	$1.08^{+0.12}_{-0.10}$	104^{+74}_{-54}	96	$1.02^{+0.04}_{-0.04}$	71^{+31}_{-28}	96	(f)

^a N constrained. See Ref. 12 for details.^b $\lambda = 56.3/150$.

both. (c) An extra term in χ^2 is added which constrains N within a Gaussian error.¹² The best-fit values of Λ^{-2} in Table I for these fits are larger than zero. The indicated errors are statistical. A drop of Λ^{-2} with imposition of the normalization constraint suggests that a significant component of the observed slope in q^2 is caused by ratios exceeding unity at low q^2 , particularly in the case of the data in Fig. 2(g).

Sensitivity of the results to variation between different analysis strategies is estimated by comparing these individual results with their average (used to produce Fig. 2). These comparisons give agreement within about 10% over the range $12 < q^2 < 35$ (GeV/c)² for 150-GeV data. The analyses are sensitive to possible biases in calibration and resolution of muon energy reconstruction, to which we currently assign a systematic error $\sigma(\Lambda^{-2}) = 20 \times 10^{-4}$ GeV⁻². Other sources of systematic error [for example, scale-noninvariance of $R(=\sigma_s/\sigma_i)$ and of radiative corrections] increase our interim overall systematic error allowance to $\sigma(\Lambda^{-2}) = 25 \times 10^{-4}$ GeV⁻² at 150 GeV.

The ratio of the 150-GeV data to the SLAC prediction does not fit the hypothesis of a constant value as a function of q^2 without severe restriction of accepted ω events. A propagator fit gives $\Lambda^{-2} > 0$ by 2.7 standard deviations (0.7% confidence level for $\Lambda^{-2} \leq 0$) when the systematic errors are added in quadrature with the statistical errors. The (150 GeV)/(56.3 GeV) and the (56.3 GeV)/(SLAC prediction) ratios also fit poorly to a constant ratio versus q^2 . The ω range for 56.3-GeV

data is identical to that at 150 GeV. Parametrizing the possible deviation of scale invariance with the propagator fit is a poor choice since the Λ^{-2} values obtained depend on the ω region included, and N tends to exceed unity.

When the fits are restricted to high q^2 and low ω , the parameter Λ is greater than 10 GeV at the 90% confidence level. Previous muon inelastic scattering experiments¹¹ set a limit $\Lambda > 5.1$ GeV [$(\Lambda^{-2} < 380) \times 10^{-4}$ GeV⁻²] with 95% confidence in comparisons with electron scattering.

The results presented here are a preliminary look at a subset of our data. The remaining scattered muons in our total sample come from other target positions and materials covering a wider range of q^2 , both lower and higher, and data in the large- ω region. The results will be reported soon. We thank L. Litt, B. Meyer, K. Rajendra, B. Thelan, and D. Chapman for their contributions. We acknowledge the assistance of R. Huson, P. Limon, R. Orr, T. Toohig, T. Yamanouchi, and other staff of the Fermi Laboratory.

*Work supported in part by the National Science Foundation.

†Deceased.

‡Now at Stanford Linear Accelerator Center, Stanford, Calif. 94305.

§Present address: Texaco Exploration Canada, Ltd., Calgary, Alta., Canada.

||Visiting Assistant Professor, Cornell University, 1971-1972. Now at the Department of Physics and

Lawrence Berkeley Laboratory, University of California, Berkeley, Calif. 94720.

¹J. D. Bjorken, Phys. Rev. 179, 1547 (1969).

²Kinematic variables used here are squared four-momentum transfer, q^2 ; incident and scattered muon energy, E_0 and E' ; $\nu = E_0 - E'$; and $\omega = 2m\nu/q^2$.

³G. Miller *et al.*, Phys. Rev. D 5, 528 (1972).

⁴R. P. Feynman, *Photon-Hadron Interactions* (Benjamin, New York, 1972).

⁵For example, radiative corrections do not scale exactly and the effect on the data/data ratio is of the order of 5%. The apparatus nonscaling correction on Λ^{-2} (defined in Table I) is estimated to be less than $20 \times 10^{-4} \text{ GeV}^{-2}$ by a Monte Carlo calculation.

⁶A. Bodek, Ph.D. thesis, Massachusetts Institute of Technology, 1973 (unpublished); A. Bodek *et al.*, Phys. Rev. Lett. 30, 1087 (1973). The agreement between the Bodek fit to νW_2 and the SLAC-MIT D_2 data (assuming $R=0.18$) is better than 6% and typically better than 2% for ω' values above 9 at all q^2 values ($> 1 \text{ GeV}^2/c^2$) measured at SLAC. J. S. Poucher *et al.*, SLAC Report No. SLAC-PUB-1309, 1973 (unpublished), and (without tables of cross sections) Phys. Rev. Lett. 32, 118 (1974). For large- ω events, use of ω' introduces insignificant changes.

nificant changes.

⁷Variation of $R (= \sigma_s/\sigma_t)$ between 0 and ∞ could give rise to changes of order 10% in the ratios in Fig. 2.

⁸The Fermi motion correction is a function of ω only. See G. B. West, Ann. Phys. (New York) 14, 464 (1972).

⁹K. W. Chen, Bull. Amer. Phys. Soc. 19, 100 (1974). The preliminary results reported correspond to Fig. 2(g).

¹⁰This agreement checks the Monte Carlo assumptions since these data are even more sensitive to the variation of acceptance in q^2 and ω than data outside the SLAC kinematic region. The enhancement of $\omega > 9$ events remains as the acceptance is varied from 12% to over 65% (by varying q^2).

¹¹A. Entenberg *et al.*, Phys. Rev. Lett. 32, 486 (1974); J. Kim *et al.*, to be published.

¹²The 150/56.3 ratio is "constrained" to 1.0 ± 0.05 . The data-to-Monte Carlo ratios are constrained to $N = 0.925 \pm 0.038$ (Ref. 11) times an estimated detection efficiency of 0.95 ± 0.10 .

¹³The acceptance is primarily defined by the maximum and minimum scattering angle and this is a function of q^2 and ω . Figure 2(e) shows the average acceptance versus q^2 .

Effect of $N^*(1236)$ on Radiative Muon Capture in Calcium

Kohichi Ohta

Institute of Physics, University of Tokyo, Komaba, Meguro-ku, Tokyo 153, Japan

(Received 19 September 1974)

Influence of the one-pion exchange current brought about by the $N^*(1236)$ excitation is considered for the photon spectrum of radiative muon capture in calcium. It is found that the relative rate of radiative to ordinary muon capture is substantially lowered and that the discrepancy between partial conservation of axial-vector current theory and experiment is removed.

A recent experiment¹ which measured the energy spectrum of the internal bremsstrahlung of radiative muon capture in calcium presents a puzzling problem. The experimental spectrum is completely inconsistent with a shell-model calculation based on the effective Hamiltonian for radiative muon capture by a free proton.² In the effective Hamiltonian the Goldberger-Treiman prediction³ is used to express the induced pseudoscalar form factor h_A in terms of the axial-vector form factor $g_A \cong 1.24$. However because of the nonconservation of the axial current, the effective g_A and h_A to be used for a nucleon bound in a nucleus cannot be the same as those for a free nucleon. Indeed it was found that in ordinary muon capture both g_A and h_A are reduced as a result of exchange current arising from the $N^*(1236)$ isobar.⁴

In this note I show that inclusion of the hitherto neglected effect of the pion exchange current removes the necessity for unfounded alteration of h_A from the partial conservation of axial-vector current (PCAC) prediction.

The matrix element for the process in which a stopped muon is absorbed while a γ ray is given off by two nucleons interacting through the exchange of a pion is obtained by inserting a photon at all possible places in the corresponding nonradiative Feynman diagram. The resulting set of diagrams is